



# Quantitative ultrasound envelope statistics imaging as a screening approach for pediatric hepatic steatosis and liver fibrosis: using biomarker and transient elastography as reference standards

Chiao-Shan Hsieh<sup>a,1</sup>, Ming-Wei Lai<sup>b,c,1</sup>, Chien-Chang Chen<sup>b</sup>, Hsun-Chin Chao<sup>b</sup>, Chiao-Yin Wang<sup>d</sup>, Yung-Liang Wan<sup>d,e</sup>, Zhuhuang Zhou<sup>f,\*\*</sup>, Po-Hsiang Tsui<sup>b,c,d,\*</sup>

<sup>a</sup> Department of Biomedical Engineering, Chang Gung University, Taoyuan, Taiwan

<sup>b</sup> Division of Pediatric Gastroenterology, Department of Pediatrics, Chang Gung Memorial Hospital at Linkou, Taoyuan, Taiwan, College of Medicine, Chang Gung University, Taoyuan, Taiwan

<sup>c</sup> Liver Research Center, Chang Gung Memorial Hospital at Linkou, Taoyuan, Taiwan

<sup>d</sup> Department of Medical Imaging and Radiological Sciences, College of Medicine, Chang Gung University, Taoyuan, Taiwan

<sup>e</sup> Department of Medical Imaging and Intervention, Chang Gung Memorial Hospital at Linkou, Taoyuan, Taiwan

<sup>f</sup> Department of Biomedical Engineering, Faculty of Environment and Life, Beijing University of Technology, Beijing, China

## ARTICLE INFO

### Keywords:

Ultrasound  
Liver  
Steatosis  
Fibrosis  
Children

## ABSTRACT

Quantitative ultrasound (QUS) envelope statistics imaging is an emerging technique for the assessment of hepatic steatosis in adults. Blood tests are currently recommended as the screening tool for pediatric hepatic steatosis, a condition that can lead to liver fibrosis in children. This study examined the utility of QUS envelope statistics imaging in grading biomarker-diagnosed hepatic steatosis and detecting liver fibrosis in a pediatric population. A total of 173 subjects was enrolled (Group A) for QUS envelope statistics imaging using two statistical distributions, Nakagami and homodyned K (HK) models, and information entropy. QUS parameter values were compared with the hepatic steatosis index (HSI) and steatosis grade (G0: HSI <30; G1: 30 ≤ HSI <36; G2: 36 ≤ HSI <41.6; G3: ≥41.6). An additional cohort of 63 subjects (Group B) was recruited to undergo both QUS envelope statistics imaging and liver stiffness measurements (LSM) obtained from the transient elastography (Fibroscan), with a cutoff value set at 5 kPa to indicate liver fibrosis. The diagnostic performances were evaluated using the area under the receiver operating characteristic curve (AUROC). QUS envelope statistics imaging generated the AUROC values for steatosis grading at levels ≥ G1, ≥ G2, and ≥ G3 ranged from 0.94 to 0.97, 0.91 to 0.93, and 0.83 to 0.87, respectively, and produced an AUROC range of between 0.82 and 0.84 for identifying liver fibrosis. QUS envelope statistics imaging integrates the benefits of both biomarkers and elastography, enabling the screening of hepatic steatosis and detection of liver fibrosis in a pediatric population.

\* Corresponding author. Department of Medical Imaging and Radiological Sciences, College of Medicine, Chang Gung University, Taoyuan, Taiwan

\*\* Corresponding author. Department of Biomedical Engineering, Faculty of Environment and Life, Beijing University of Technology, Beijing, China

E-mail addresses: [zhouzh@bjut.edu.cn](mailto:zhouzh@bjut.edu.cn) (Z. Zhou), [tsuiph@mail.cgu.edu.tw](mailto:tsuiph@mail.cgu.edu.tw) (P.-H. Tsui).

<sup>1</sup> These authors contributed equally to this work.

<https://doi.org/10.1016/j.heliyon.2023.e22743>

Received 29 October 2023; Received in revised form 16 November 2023; Accepted 17 November 2023

Available online 23 November 2023

2405-8440/© 2023 The Authors. Published by Elsevier Ltd. This is an open access article under the CC BY-NC-ND license (<http://creativecommons.org/licenses/by-nc-nd/4.0/>).

## 1. Introduction

Nonalcoholic fatty liver disease (NAFLD) affects approximately 25 % of the global population [1] and is emerging as one of the most prevalent chronic liver diseases among both adults and children [2]. The prevalence of NAFLD in children is estimated to range from 7.6 % in the general pediatric population to 34.2 % in the obese pediatric population [3]. About 11 % of children with obesity develop advanced fibrosis [4]. Furthermore, a recent study discovered that 60 % of obese children have liver fibrosis due to significant hepatic steatosis [5]. Grading hepatic steatosis and predicting liver fibrosis in children are essential for maintaining healthy liver function through appropriate interventions.

Liver biopsy is the gold standard for grading hepatic steatosis. Magnetic resonance imaging (MRI) and ultrasound are commonly used noninvasive methods for diagnosing hepatic steatosis [2]. MRI-based proton density fat fraction (PDFF) can differentiate between histological grades of steatosis and has become a standard method for quantifying steatosis [2]. However, MRI equipment is not universally available, posing a challenge for community-based screenings. In contrast, ultrasound is a more child-friendly method for diagnosing hepatic steatosis due to its real-time nature and widespread availability. Nonetheless, detecting mild steatosis with ultrasound can be challenging and has lower accuracy [6].

Quantitative ultrasound (QUS) has gained widespread acceptance as a solution to the deficiencies of conventional ultrasound B-scan in characterizing tissues [6]. Since hepatic steatosis is clinically identified by histopathological evidence [7], QUS techniques that can provide microstructural information may be preferable for application in the diagnosis of hepatic steatosis. Among all possibilities, QUS envelope statistics imaging is gaining attention and has been recommended for the assessment of hepatic steatosis [8,9]. The envelope statistics refers to the statistical distribution of ultrasound backscattered envelope signals (i.e., the echo amplitude distribution). Studies have shown that backscattered signals vary with microstructures, and modeling the echo amplitude distribution enables tissue characterization [10]. Currently, the Nakagami distribution, homodyned K (HK) distribution, and information entropy are commonly employed methods for describing the backscattered statistics of the liver [11]; their parameters and QUS imaging methodologies have been histologically shown to correlate with hepatic steatosis in adult populations [12–14]. Due to less computational complexity, ultrasound Nakagami parametric imaging is already commercially available as a medical device for clinical use, such as AmCAD-US software (AmCad BioMed Corp.) and tissue scatter distribution imaging (TSI™, Samsung Medison). A previous study used AmCAD-US to assess pediatric hepatic steatosis using Nakagami imaging, demonstrating that envelope statistics are sensitive to the level of fatty liver in children [15]. Nakagami imaging also showed good intra- and inter-observer agreements (intraclass correlation coefficient, 0.98 and 0.95, respectively) [9].

While QUS envelope statistics imaging is a well validated tool in assessing hepatic steatosis, some key issues in pediatric clinical practice warrant further investigation. Firstly, according to the clinical practice guidance issued by the North American Society of Pediatric Gastroenterology, Hepatology, and Nutrition (NASPGHAN), biomarkers derived from blood tests are still recommended for screening pediatric NAFLD, as they yield vital insights into hepatic steatosis [16]. Earlier validations of QUS envelope statistics imaging focused on histological evidence comparisons. Nevertheless, in line with NASPGHAN's recommendations, investigating the correlation between QUS envelope statistics imaging and hepatic steatosis biomarkers might enhance the diagnostic applicability of ultrasound in the pediatric population by establishing connections with the biochemical alterations caused by fatty liver disease. Second, considering that children with hepatic steatosis could develop liver fibrosis, it is crucial to explore whether QUS envelope statistics imaging could both grade hepatic steatosis and potentially identify the existence of liver fibrosis. The impact of various statistical models on the performance of QUS envelope statistics imaging in characterizing pediatric hepatic steatosis and liver fibrosis also needs to be explored.

This study aims to assess the diagnostic potential of QUS envelope statistics imaging, leveraging Nakagami, HK, and entropy methodologies, in the screening of pediatric hepatic steatosis, with biomarkers serving as the reference standard. Additionally, this study seeks to further evaluate the feasibility of these proposed methodologies in the detection of liver fibrosis in a pediatric population.

## 2. Materials and methods

### 2.1. Participants

This study was approved by the institutional review board (IRB) of Chang Gung Memorial Hospital. All participants and their parents (or legal representatives) provided written informed consent. Subject enrollment was carried out in two successive stages.

The experiments in the first and second stages were carried out independently at different time intervals. In the first stage, a total of 173 subjects were enrolled (no. 201800983B0; approval date: July 12, 2018). The inclusion criteria targeted individuals aged 3–18 years who were scheduled for abdominal ultrasound examinations, including (i) subjects with a body mass index (BMI) < 85th percentile and without imaging findings of hepatic steatosis (defined as the normal control) and (ii) overweight or obese patients with a BMI ≥85th percentile and suspected hepatic steatosis due to increased hepatic echogenicity. Those with secondary obesity conditions, current medication use, or coexisting chronic or acute illnesses were excluded. Notably, although diabetes mellitus (DM) could be considered as an exclusion criterion, it is essential for calculating hepatic steatosis biomarkers in this study (refer to section 2.3 for details). Therefore, DM was not used as an exclusion criterion. In the second stage, 21 normal subjects and 42 patients were recruited (no. 201901920B0; approval date: January 8, 2020) under the same inclusion and exclusion criteria. The dataset obtained in the first stage ( $n = 173$ , denoted by Group A) was leveraged to evaluate the efficacy of QUS envelope statistics imaging in grading pediatric

hepatic steatosis, and those amassed in the second stage ( $n = 63$ , denoted by Group B) was employed to assess the feasibility of the proposed methodologies in detecting liver fibrosis in children. Based on power analysis performed with  $G \times Power$  software (version 3.1, Heinrich-Heine-University, Düsseldorf, Germany), the sample sizes are sufficient to achieve a power of 0.85 given an effect size of 0.5 and a significance level ( $\alpha$ ) of 0.15. The process of study population selection is graphically represented in Fig. 1. Notably, we directly excluded subjects meeting the exclusion criteria in this study, and thus specific counts of the excluded cases were unavailable.

2.2. Anthropometric, blood tests, and fibroscan measurements

In Group A, anthropometric indices were recorded for each participant, and after an overnight fast of 8 h, blood tests were conducted to measure aspartate aminotransferase (AST) and alanine aminotransferase (ALT) levels. In Group B, in addition to the same anthropometric and blood test assessments used in Group A, transient elastography (Fibroscan®, Echosens) was additionally used to perform liver stiffness measurement (LSM) on the patients [17]. In a supine position, LSM was measured through the intercostal spaces with an M probe targeting the right hepatic lobe. A reliable examination must consist of at least 10 measurements with a success rate of >60 % and an interquartile median ratio that is <30 % of the median values of LSM [18]. The final LSM were recorded as the median value of all measurements.

2.3. Assessment of pediatric hepatic steatosis and liver fibrosis

Hepatic steatosis index (HSI) and LSM were used as the diagnostic benchmarks for hepatic steatosis and liver fibrosis, respectively. HSI is a biomarker calculated by  $8 \times (ALT/AST) + BMI$  (+2 if female; +2 if diagnosed as having DM) [19] that holds significant histopathological significance [19,20]. HSI values greater than 41.6 and 43 indicate mild ( $\geq 5\%$ ) and moderate to severe ( $\geq 33\%$ ) histological steatosis, respectively [20]. An HSI value less than 30 rules out the possibility of hepatic steatosis, while an HSI value greater than 36 indicates its presence [19]. In Group A, the hepatic steatosis grade was determined based on the HSI cutoff values listed below: grade 0 (G0:  $HSI < 30$ ), grade 1 (G1:  $30 \leq HSI < 36$ ), grade 2 (G2:  $36 \leq HSI < 41.6$ ), and grade 3 (G3:  $HSI \geq 41.6$ ) [15]. On the other hand, a normal liver LSM value for children is around 4 kPa [21,22], and LSM values greater than or equal to 5 kPa suggest the presence of any fibrosis ( $\geq$  Metavir score F1) [23]. Therefore, in Group B, the cutoff LSM  $\geq 5$  kPa was chosen to represent pediatric liver fibrosis.

2.4. Ultrasound data acquisition for QUS envelope statistics imaging

Each subject underwent ultrasound scanning using a clinical system (Model 3000, Terason) and a 3.5-MHz convex transducer with

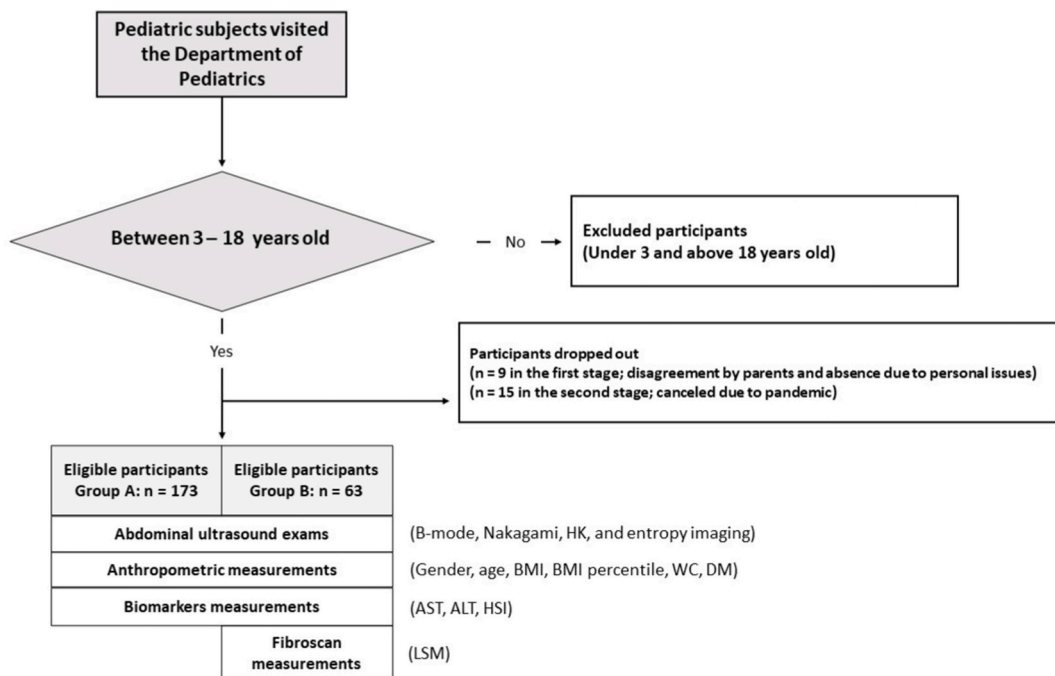
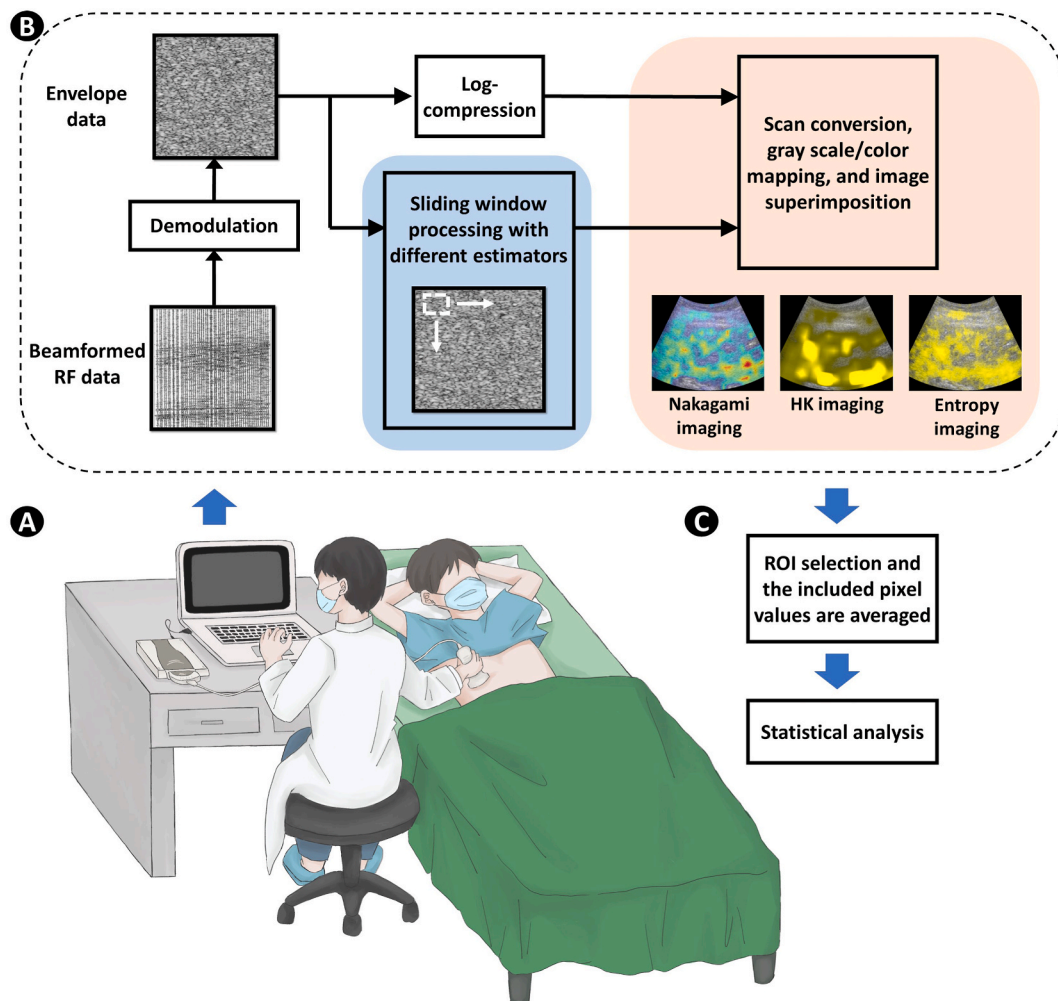


Fig. 1. Study enrollment chart. A total of 173 and 63 subjects were enrolled in Groups A and B, respectively. In Group A, the diagnostic performances of the proposed QUS envelope statistics techniques in grading pediatric hepatic steatosis were explored. In Group B, the performances in detecting liver fibrosis in children were investigated.

a pulse length of 2.3 mm (Model 5C2A, Terason). The imaging focus was at 4 cm, and the depth was 8 cm. Three independent intercostal scans were performed on the liver parenchyma (segment VIII) by a pediatric gastroenterologist who was blinded to the subjects' medical histories and clinical findings. Each scan must be effective, defined as being devoid of acoustic shadowing effects or significant vascular structures. Based on a previous study [24], intercostal scanning is an appropriate imaging plane for analyzing backscattering in the liver. At the breath-hold moment during gentle, normal respiration, each raw image data, comprised of 256 scan lines of beamformed radiofrequency (RF) signals, were captured and stored for offline processing using MATLAB software (version R2019a, MathWorks). The corresponding envelope image was derived by calculating the absolute value of the Hilbert transform applied to each RF signal, thus describing the echo amplitude. Ultrasound B-mode imaging was presented using the log-compressed envelope of the raw image data. QUS envelope statistics imaging was subsequently constructed by applying a sliding window processing technique to the uncompressed envelope image, with the Nakagami parameter  $m$  of the Nakagami distribution (estimated using the moment estimator to depict envelope statistics varying from pre-Rayleigh to post-Rayleigh distributions), the scatterer clustering parameter  $\mu$  of the HK distribution (estimated using the XU estimator to measure the number of scatterers per resolution cell), and the entropy value (estimated using the histogram method to describe the signal uncertainty) [12,13]. The window overlapping ratio was 50% [25], and the side lengths of the window for Nakagami, HK, and entropy parametric imaging were set at three [12], five [26], and one [12,25] times the pulse length of the transducer, respectively. The Nakagami, HK, and entropy images were superimposed on B-mode images to display both structural and parametric information through pseudocolor coding. A range of Nakagami parameter from 0 to 2 corresponded to a color transition from blue to red; HK parameter ranging from 0 to 5 showed an increasing intensity of yellow; and for entropy parameters, a range from 5.2 to 5.3 also corresponded to an increasing intensity of yellow. The algorithmic scheme of QUS envelope statistics imaging was illustrated in Fig. 2a–(c).



**Fig. 2.** The algorithmic scheme of QUS envelope statistics imaging. (a) Ultrasound intercostal scanning is performed; (b) raw image data is acquired for QUS envelope statistics imaging using the sliding window processing; (c) ROI selection for quantitative analysis.

## 2.5. Statistical analysis

The values of the Nakagami, HK, and entropy measures of each subject were obtained by averaging the pixel values in QUS envelope statistics images corresponding to the regions of interest (ROIs) of the acquired three B-mode images. The ROIs were manually defined by a radiologist with extensive knowledge of imaging anatomy. The primary guideline for ROI selection was to exclusively encompass the liver parenchyma, excluding any non-liver parenchymal regions, to minimize bias in envelope statistics measurements. The parameters were plotted as medians and interquartile ranges (IQR). An independent *t*-test and a one-way analysis of variance (ANOVA) were used to compare the data. Multiple comparisons were conducted using the Holm-Sidak method. Kruskal-Wallis ANOVA was used in case the data set did not pass the normality test, and Dunn's test was used for multiple comparisons. To evaluate the diagnostic performance, the receiver operating characteristic (ROC) curve was used. The area under the ROC curve (AUROC) and other statistical results were reported. The DeLong test was used to compare the ROC curves and identify significant differences. All statistical analyses were performed using SigmaPlot (version 12.0, Systat Software, Inc., CA, USA). Statistical significance was set at  $p < 0.05$ .

## 3. Results

### 3.1. Demographic data

Group A consisted of 173 subjects; the age was  $11.96 \pm 3.95$  years old, BMI was  $25.51 \pm 6.94$  kg/m<sup>2</sup>, and the waist circumference (WC) was  $83.41 \pm 19.44$  cm. Group B consisted of 63 subjects; the age was  $13.30 \pm 2.81$  years old, BMI was  $25.93 \pm 5.72$  kg/m<sup>2</sup>, and WC was  $85.62 \pm 16.65$  cm. Demographic data are presented in Table 1.

### 3.2. QUS envelope statistics imaging of hepatic steatosis

B-scan images increased in brightness with increasing hepatic steatosis grade; meanwhile, the shading of QUS envelope statistics images varied accordingly (Fig. 3a–(d)). The median values and IQRs of the Nakagami parameter increased from 0.61 (IQR: 0.57–0.65) to 0.87 (IQR: 0.86–0.89) as steatosis grade increased from G0 to G3 ( $p < 0.05$ ; Fig. 4a). Within the same range of steatosis grade, the HK parameter and entropy value increased from 1.37 (IQR: 1.17–1.77) to 4.11 (IQR: 3.60–4.72) ( $p < 0.05$ ; Figs. 4b) and 5.19 (IQR: 5.18–5.21) to 5.26 (IQR: 5.25–5.27) ( $p < 0.05$ ; Fig. 4c), respectively. Using the Nakagami, HK, and entropy values, the AUROCs for grading biomarker-diagnosed pediatric hepatic steatosis  $\geq$  G1 were 0.96, 0.94, and 0.97, respectively (Fig. 4d). When grading steatosis  $\geq$  G2, the AUROCs were around 0.9 (Fig. 4e). The AUROCs ranged from 0.83 to 0.87 (Fig. 4f) when grading steatosis  $\geq$  G3. A summary of performance evaluation are presented in Table 2.

### 3.3. QUS envelope statistics imaging of liver fibrosis

QUS envelope statistics imaging not only varied with pediatric hepatic steatosis but also exhibited enhanced brightness due to liver fibrosis in children (Fig. 5a–(d)). The Nakagami, HK, and entropy values (median, IQR) of the fibrosis group (LSM  $\geq$  5 kPa) are (0.84, 0.75–0.91), (7.16, 3.93–9.55), and (5.24, 5.21–5.26), respectively, all of which were higher than those of the normal control group ( $p < 0.05$ ; Fig. 6a, b, c, and Table 3). AUCROC values for evaluating liver fibrosis were 0.82, 0.84, and 0.83, respectively, for the Nakagami parameter, HK parameter, and entropy value (Fig. 6d and Table 4). AUROCs between Nakagami, HK, and entropy imaging

**Table 1**

Demographic data of the participants enrolled in Group A and Group B. Data are expressed by mean  $\pm$  standard deviation (range) and median.

Demographics	Group A		Group B	
n	173		63	
Male	118 (68 %)		46 (73.02 %)	
Female	55 (32 %)		17 (26.98 %)	
Age (years)	$11.96 \pm 3.95$ (3.00–17.00)	13.00	$13.30 \pm 2.81$ (6.00–17.00)	14.00
BMI (kg/m <sup>2</sup> )	$25.51 \pm 6.94$ (11.42–43.15)	25.43	$25.93 \pm 5.72$ (13.82–43.15)	25.71
BMI percentiles, %	$81.56 \pm 26.09$ (2.00–99.00)	96.00	$81.89 \pm 24.58$ (10.00–99.00)	97.00
WC (cm)	$83.41 \pm 19.44$ (46.50–126.00)	87.00	$85.62 \pm 16.65$ (57.00–126.00)	91.00
DM	7 (4.05 %)		3 (5.56 %)	
<b>Laboratory</b>				
AST (U/L)	$42.86 \pm 32.19$ (15.00–250.00)	32.00	$35.86 \pm 20.82$ (15.00–116.00)	30.00
ALT (U/L)	$70.80 \pm 96.81$ (5.00–769.00)	37.00	$60.11 \pm 58.35$ (5.00–256.00)	40.00
<b>Hepatic steatosis index</b>				
HSI	$37.07 \pm 11.88$ (17.80–80.05)	27.99	$38.02 \pm 11.41$ (19.02–64.19)	37.61
<b>Fibroscan</b>				
LSM (kPa)			$5.85 \pm 2.19$ (2.70–13.90)	5.60

Note—Unless otherwise noted, data are numbers of patients. BMI: body mass index, WC: waist circumference, DM: diabetes mellitus, AST: aspartate aminotransferase, ALT: alanine aminotransferase, HSI: hepatic steatosis index, LSM: liver stiffness measurement. Laboratory normal range of AST in children between 2 and 18 y/o is 13–40 U/L. Laboratory normal range of ALT in children between 1 and 18 y/o is 7–40 U/L.

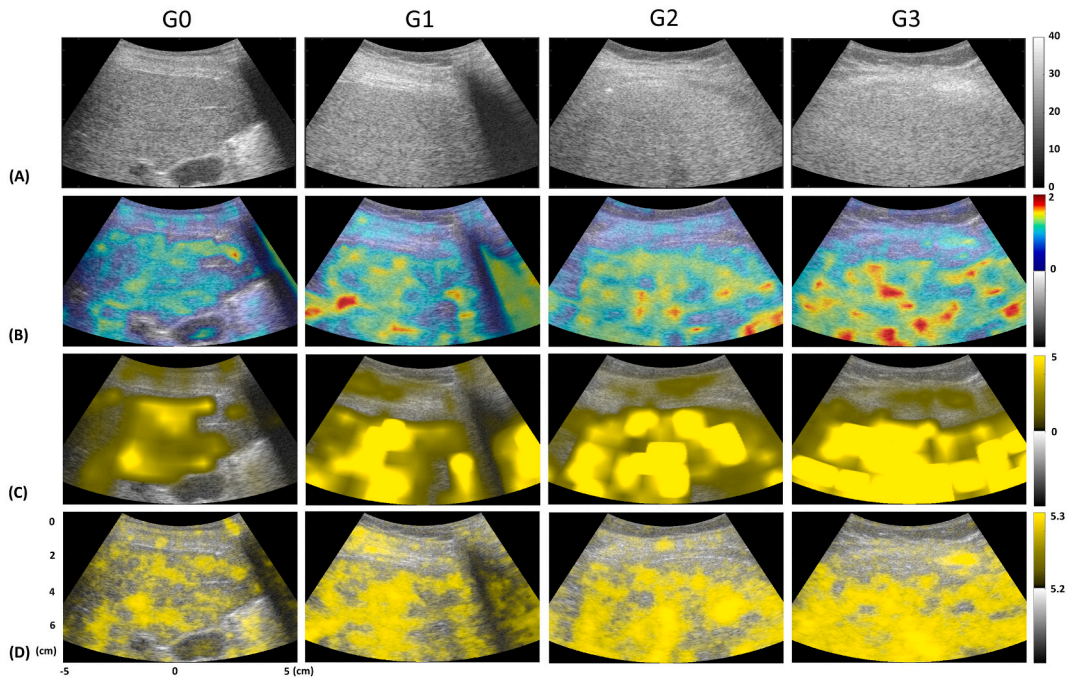


**Fig. 3.** Ultrasound B-mode and QUS envelope statistics images for different grades of pediatric hepatic steatosis. (a) Ultrasound B-scan; (b) Nakagami; (c) HK; (d) entropy images. QUS envelope statistics images varied with increasing the grade of hepatic steatosis.

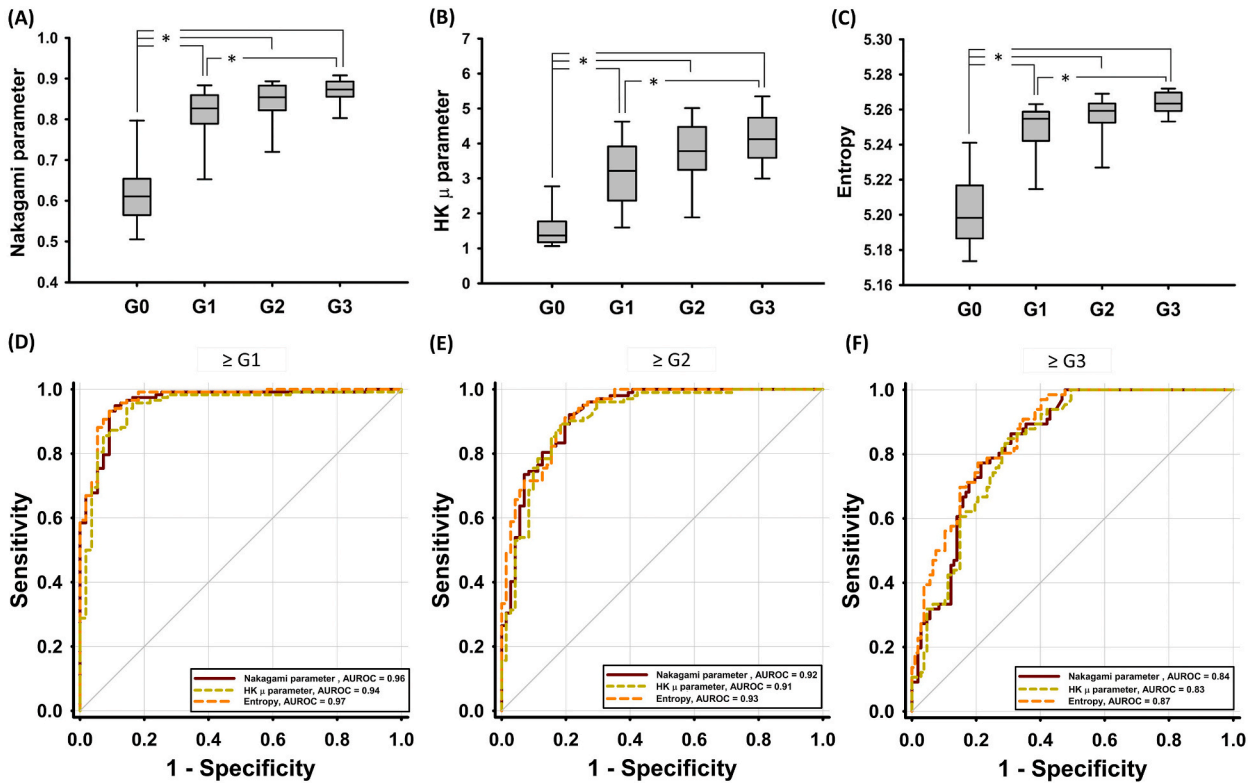


**Fig. 4.** (a)–(c) QUS envelope statistics imaging parameters as a function of hepatic steatosis grade. The Nakagami, HK, and entropy values increased when the steatosis grade increased from G0 to G3 (\*:  $p < 0.05$ ); (d)–(f) the ROC curves for using the Nakagami, HK, and entropy values to grade pediatric hepatic steatosis. AUROC ranged from 0.94 to 0.97.

**Table 2**

Comparisons of data in each grade of hepatic steatosis (data are expressed by the median values and the IQRs) and performance evaluation. QUS envelope statistics imaging had an outstanding performance in grading pediatric hepatic steatosis. There were no significant differences in the performances for grading G1, G2, and G3 among the Nakagami, HK, and entropy methods ( $p > 0.05$ ).

	The grade of hepatic steatosis				p value (ANOVA)
	G0	G1	G2	G3	
<b>n</b>	55	16	36	66	
<b>HSI</b>	21.98 (20.05–26.27)	33.53 (33.02–35.50)	38.35 (37.10–39.82)	48.36 (43.74–51.93)	$p < 0.05$
<b>Nakagami parameter</b>	0.61 (0.57–0.65)	0.83 (0.79–0.86)	0.86 (0.82–0.88)	0.87 (0.86–0.89)	$p < 0.05$
<b>HK <math>\mu</math> parameter</b>	1.37 (1.17–1.77)	3.22 (2.36–3.91)	3.81 (3.26–4.53)	4.11 (3.60–4.72)	$p < 0.05$
<b>Entropy</b>	5.19 (5.18–5.21)	5.25 (5.24–5.26)	5.26 (5.25–5.26)	5.26 (5.25–5.27)	$p < 0.05$

Parameter	$\geq G1$			$\geq G2$			$\geq G3$		
	Nakagami parameter	HK $\mu$ parameter	Entropy	Nakagami parameter	HK $\mu$ parameter	Entropy	Nakagami parameter	HK $\mu$ parameter	Entropy
<b>Cutoff value</b>	0.78	2.65	5.24	0.80	3.06	5.25	0.85	3.48	5.26
<b>AUROC</b>	0.96	0.94	0.97	0.92	0.91	0.93	0.84	0.83	0.87
<b>Accuracy (%)</b>	92.50	88.40	92.50	85.50	85.50	86.10	78.00	75.70	78.00
<b>Sensitivity (%)</b>	90.90	90.90	90.90	80.30	83.10	81.70	78.50	72.00	78.70
<b>Specificity (%)</b>	93.20	87.30	93.20	89.20	87.30	89.20	77.30	81.80	76.90
<b>Youden index</b>	0.84	0.78	0.84	0.70	0.70	0.71	0.56	0.54	0.56
<b>SE</b>	0.02	0.02	0.02	0.02	0.03	0.02	0.03	0.03	0.03
<b>LR +</b>	13.40	7.20	13.40	7.40	6.50	7.60	3.50	4.0	3.40
<b>LR-</b>	0.10	0.10	0.10	0.20	0.20	0.20	0.30	0.30	0.30
<b>PPV (%)</b>	86.20	76.90	86.20	83.80	81.90	84.10	84.80	86.50	85.00
<b>NPV (%)</b>	95.70	95.40	95.70	86.70	88.10	87.50	68.90	64.30	68.50

Note—Unless otherwise noted, data are numbers of patients. HSI: hepatic steatosis index. The severity of pediatric hepatic steatosis was graded on the basis of the range of the HSI values as grade 0 (G0: HSI <30), grade 1 (G1: 30 ≤ HSI <36), grade 2 (G2: 36 ≤ HSI <41.6), grade 3 (G3: 41.6 ≤ HSI). AUROC: area under the receiver operating characteristic (ROC) curve, SE: standard error, LR+: positive likelihood ratio, LR-: negative likelihood ratio, PPV: positive predictive value, NPV: negative predictive value.

were not significantly different ( $p > 0.05$ ).

#### 4. Discussion

Pediatric NAFLD is characterized by macrovesicular hepatocellular steatosis, portal inflammation, and portal fibrosis without ballooning [27,28], illustrating its histological similarity with adult NAFLD. As previously noted, alterations in envelope statistics have been histologically evidenced to vary with hepatic steatosis in adults [12–14], leading to the expectation of a corresponding relationship with steatosis in the pediatric liver. Given that fatty droplets contribute significantly to ultrasound backscattering in the liver, there exist two prevalent interpretations regarding the dependency of ultrasound backscattering and envelope statistics on liver histology. First, fat droplet accumulation in hepatocytes modifies the positions of hepatocyte nuclei, thereby altering their spatial distribution and leading to changes in the structure function and backscatter coefficient [29]. Second, hepatic steatosis transpires when fat infiltration occurs in the liver parenchyma, augmenting the quantity of random scatterers (fat-infiltrated hepatocytes) and leading to constructive wave interference. This consequently incites a shift in backscattered envelope statistics towards Rayleigh distributions [26]. As a result, Nakagami, HK, and entropy values escalate with hepatic steatosis grade, mirroring changes in echo amplitude distribution and backscattered signal uncertainty, as substantiated by the experimental data in Group A.

In Group B, most of the subjects exhibiting an LSM ≥5 kPa were diagnosed with G3 steatosis (HSI ≥41.6). This suggests a robust association between the presence of liver fibrosis and the severity of hepatic steatosis in pediatric subjects, and notably, the underlying mechanism may be obesity. In a study involving pediatric patients with varying degrees of obesity, liver stiffness was found to increase with obesity severity [30]. Evidence suggests that obesity leads to stiffer livers, as some researchers have observed significantly higher shear wave velocity values in children with obesity [31]. Hepatic steatosis indeed fosters a conducive environment in a child’s liver for the emergence of fibrosis, especially in overweight and obese children who typically exhibit substantial hepatic steatosis and early liver fibrosis. While liver fibrosis may influence ultrasound envelope statistics [32], significant hepatic steatosis—which physically results in an increased number of fatty droplets—serves as a more dominant mechanism that drives alterations in tissue microstructures and the corresponding ultrasound envelope statistics. This understanding provides the basis for why QUS envelope statistics imaging is effectively employed for identifying liver fibrosis in children.

Establishing the relationship between QUS envelope statistics imaging, the biomarker HSI, and transient elastography-based LSM presents a notable and significant finding in this study. HSI incorporates four elements: AST/ALT, BMI, gender, and the presence of diabetes mellitus. Within the liver, ALT is localized in the cellular cytoplasm, while AST is in both cytosolic and mitochondrial. Increased serum levels of these enzymes typically signify hepatocellular damage [33]. Both BMI and the presence of diabetes mellitus serve as markers of obesity and metabolic syndrome. LSM reflects steatosis-induced changes in the mechanical properties of the liver.

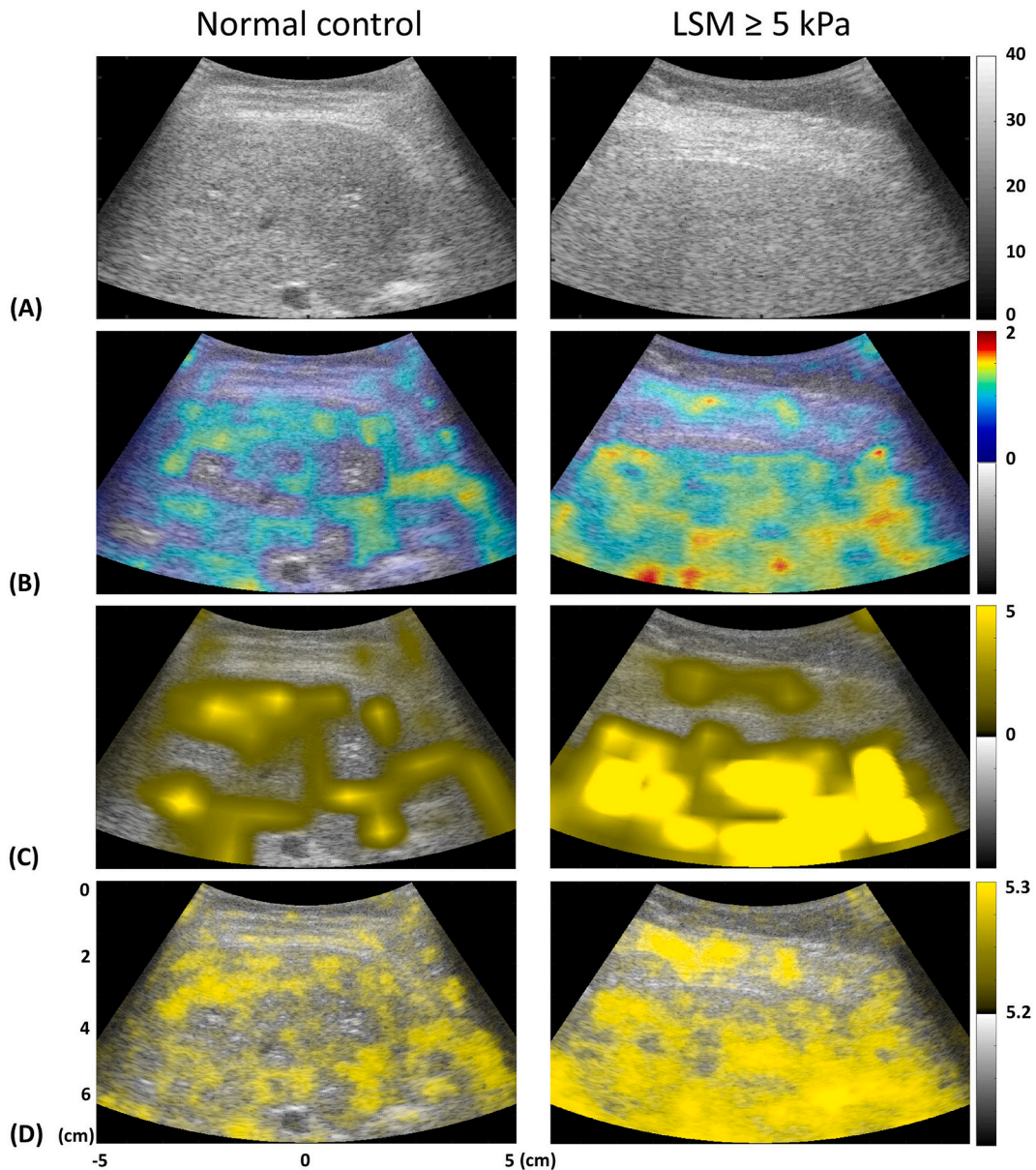


**Fig. 5.** Ultrasound B-mode and QUS envelope statistics images for the normal control and fibrosis groups. (a) Ultrasound B-scan; (b) Nakagami; (c) HK; (d) entropy images. The QUS envelope statistics images corresponding to liver fibrosis ( $LSM \geq 5$  kPa) exhibited enhanced brightness compared with those of the normal control.

According to the above viewpoints, QUS envelope statistics imaging not only links to the properties of liver microstructures but also encapsulates several crucial clinical implications, including liver injury associated with hepatic steatosis, obesity, and metabolic syndrome. As serum biomarkers for liver steatosis continue to garner substantial attention [34], QUS envelope statistics imaging could offer a fresh perspective, bridging imaging and biochemical interpretations of pediatric hepatic steatosis. More importantly, QUS envelope statistics imaging is computationally less complex and has proven feasible for real-time screening and analysis on clinical machines [9]. Compared to biomarkers, ultrasound provides routine, noninvasive assessments, and long-term follow-up of liver diseases, obviating frequent blood tests in the pediatric population. Here, to promote understanding and familiarize clinical researchers with QUS envelope statistics imaging, we have summarized the methods employed in this study in Table 5.

Another aspect warranting discussion is the interplay between the cutoff values derived from each envelope statistics model for grading pediatric hepatic steatosis and liver fibrosis. In this study, the cutoff value of the Nakagami parameter for detecting liver fibrosis fell between those for grading steatosis G2 and G3 (0.80 for grading  $\geq$  G2, 0.81 for detecting fibrosis, 0.85 for grading  $\geq$  G3). The cutoff value of the HK parameter for identifying liver fibrosis was greater than that for diagnosing steatosis G3 (3.48 for grading  $\geq$

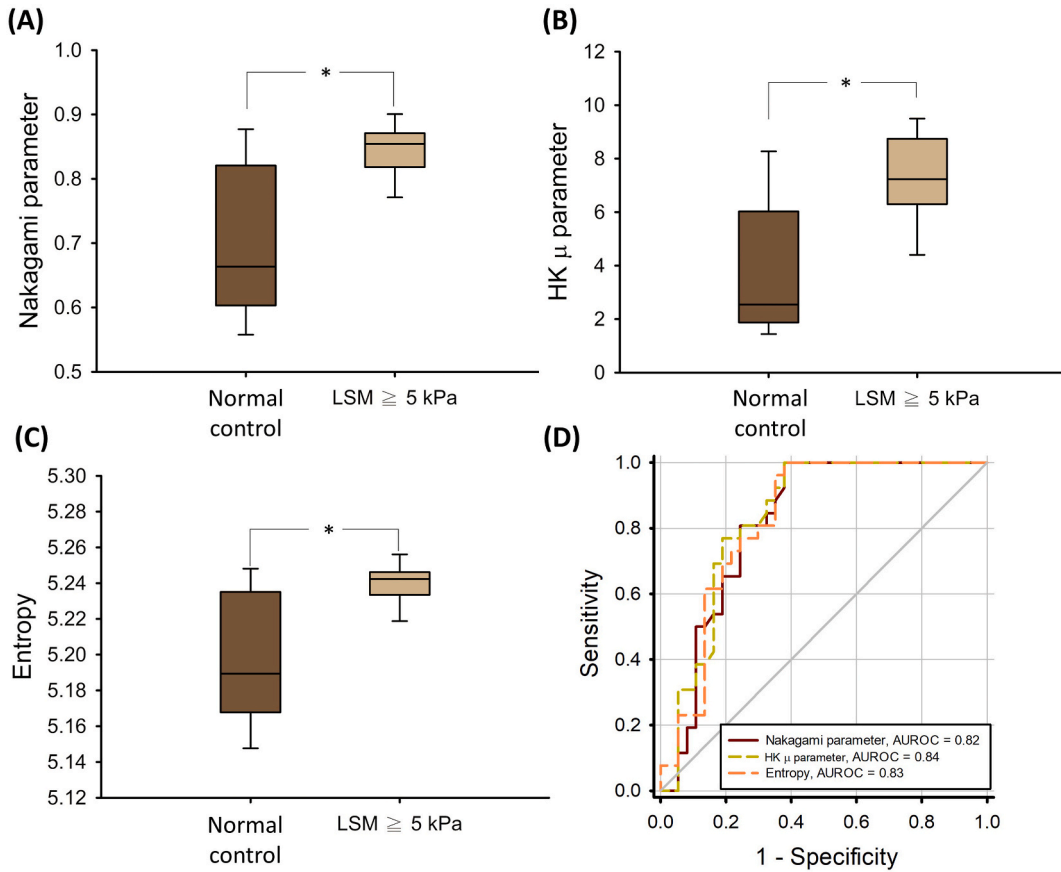


**Fig. 6.** (a)–(c) QUS envelope statistics parameters as a function of liver fibrosis. The Nakagami, HK, and entropy values of the fibrosis group (LSM ≥ 5 kPa) were higher than those of the normal control (\*:  $p < 0.05$ ); (d) the ROC curves for using the Nakagami, HK, and entropy values to detect liver fibrosis. AUROC ranged from 0.82 to 0.84.

**Table 3**

Comparisons of data between normal and fibrosis (LSM ≥ 5 kPa) groups. Data are expressed by the median and the IQRs.

LSM (kPa)	Normal control				≥5			<i>p</i> value (ANOVA)
<i>n</i>	37 (58.73 %)				26 (41.27 %)			
<b>Grades of steatosis</b>	G0	G1	G2	G3	G1	G2	G3	
<b><i>n</i> of each grade</b>	21	0	3	13	0	2	24	
LSM	3.94 (2.70–4.70)				7.02 (5.00–13.90)			$p < 0.05$
HSI	31.73 (19.02–54.82)				46.99 (35.67–64.19)			$p < 0.05$
Nakagami parameter	0.71 (0.53–0.95)				0.84 (0.75–0.91)			$p < 0.05$
HK μ parameter	4.07 (1.34–12.99)				7.16 (3.93–9.55)			$p < 0.05$
Entropy	5.20 (5.14–5.25)				5.24 (5.21–5.26)			$p < 0.05$

Note—Unless otherwise noted, data are numbers of patients. LSM: liver stiffness measurement, HSI: hepatic steatosis index. The severity of pediatric hepatic steatosis was graded on the basis of the range of the HSI values as grade 1 (G1:  $30 \leq \text{HSI} < 36$ ), grade 2 (G2:  $36 \leq \text{HSI} < 41.6$ ), grade 3 (G3:  $41.6 \leq \text{HSI}$ ).

G3, 6.23 for detecting fibrosis), while the cutoff entropy value for detecting liver fibrosis was less than that for diagnosing steatosis G1 (5.23 for detecting fibrosis, 5.24 for grading ≥ G1). In comparison, the interrelation of the cutoff values of the HK parameter for diagnosing both steatosis and liver fibrosis seem to better represent the reality that hepatic steatosis progresses to liver fibrosis in the pediatric population, thereby reflecting stronger physical significance in clinical diagnosis. Indeed, the superiorities of the HK parameter over the other parameters equip ultrasound imaging with the capability to physically describe the number density of scatterers per resolution cell, the uniformity of scattering cross-sections, and the size of fat droplets [26].

This study has some limitations. First, our study was executed in two stages. Future work would benefit from a clinical validation utilizing a single, complete dataset. Second, this study focuses on the dependency of QUS envelope statistics imaging on biomarker-diagnosed pediatric hepatic steatosis and elastography-confirmed liver fibrosis. The statistical significance and diagnostic cutoff values

**Table 4**

Performance evaluation of different ultrasound parameters in detecting pediatric liver fibrosis. QUS envelope statistics imaging produced an AUROC value of between 0.82 and 0.84 for identifying liver fibrosis. There were no significant differences in the performance among the Nakagami, HK, and entropy methods ( $p > 0.05$ ).

Parameter	Nakagami parameter	HK $\mu$ parameter	Entropy
Cutoff value	0.81	6.23	5.23
AUROC	0.82	0.84	0.83
Accuracy (%)	77.80	79.40	76.20
Sensitivity (%)	75.70	81.10	75.70
Specificity (%)	80.80	76.90	76.90
Youden index	0.56	0.58	0.53
SE	0.05	0.05	0.05
LR+	3.90	3.50	3.30
LR-	0.30	0.20	0.30
PPV (%)	84.80	83.30	82.40
NPV (%)	70.00	74.10	69.00

Note—AUROC: area under the receiver operating characteristic (ROC) curve, SE: standard error, LR+: positive likelihood ratio, LR-: negative likelihood ratio, PPV: positive predictive value, NPV: negative predictive value.

**Table 5**

Frequently employed methods for QUS envelope statistics imaging in liver tissue characterization. Compared to conventional B-scan and texture analysis, which are system-dependent, QUS envelope statistics imaging analyzes raw image data and is less influenced by system settings and operator variations. This allows for more consistent quantitative information related to scatterer properties within tissues. Furthermore, QUS envelope statistics imaging, when used for ultrasound tissue characterization, has been shown to be less influenced by liver inflammation than ultrasound elastography [35].

Method	Parameter used for imaging	Data used for parameter estimation	Physical significance
Nakagami distribution	Nakagami parameter $m$	Uncompressed backscattered envelope	Scatterer concentration
Homodyned K distribution	Scatterer clustering parameter $\mu$	Uncompressed backscattered envelope	The number of scatterers per resolution cell
Information entropy	Entropy value	Any type of ultrasound data can be used without the need to consider its statistical properties. Raw RF data or uncompressed envelope are recommended to reduce the effects of system settings and data processing.	Uncertainty or complexity of ultrasound signals

can be more accurately determined by employing gold standards (e.g., MRI-PDFF or liver biopsy) in the future. Third, this study employed 5 kPa as a cutoff value for identifying liver fibrosis. Higher cutoff values were not explored due to the limited sample size, which could introduce bias in performance evaluation from data imbalance during binary classification. Another practical consideration is the difficulty in finding advanced liver fibrosis, which corresponds to higher LSM, in subjects aged between 3 and 18 years. Finally, the proposed QUS envelope statistics imaging for assessing liver fibrosis might be exclusively applicable to children. Examining adults with more complex mechanisms in fibrosis development remains a formidable challenge.

## 5. Conclusions

This study elucidates the clinical utility of QUS envelope statistics imaging in the screening of pediatric NAFLD, focusing on issues of hepatic steatosis and liver fibrosis. The results showed that QUS envelope statistics imaging exhibited impressive diagnostic performance for pediatric hepatic steatosis using the biomarker HSI as the reference standard. Moreover, the proposed QUS strategy also allowed detection of elastography-confirmed liver fibrosis in children. This study represents the inaugural demonstration that QUS envelope statistics imaging amalgamates the benefits of both biomarkers and elastography for the comprehensive characterization of hepatic steatosis and liver fibrosis within a pediatric cohort.

## Data availability statement

Data will be made available on request.

## CRedit authorship contribution statement

**Chiao-Shan Hsieh:** Writing – original draft, Validation, Methodology, Investigation, Formal analysis. **Ming-Wei Lai:** Writing – review & editing, Resources, Investigation, Data curation, Conceptualization. **Chien-Chang Chen:** Resources, Investigation, Formal analysis, Data curation. **Hsun-Chin Chao:** Resources, Investigation, Formal analysis, Data curation. **Chiao-Yin Wang:** Validation, Software. **Yung-Liang Wan:** Writing – review & editing, Resources. **Zhuhuang Zhou:** Writing – review & editing, Software, Resources, Methodology, Funding acquisition. **Po-Hsiang Tsui:** Writing – review & editing, Supervision, Project administration,

Methodology, Funding acquisition, Conceptualization.

### Declaration of competing interest

The authors declare that they have no known competing financial interests or personal relationships that could have appeared to influence the work reported in this paper.

### Acknowledgements

This work was supported by National Science and Technology Council in Taiwan (NSTC 112-2221-E-182 -006-MY3) and Chang Gung Memorial Hospital (CMRPD1N0011, CMRPD1M0401). This work was supported in part by Beijing Natural Science Foundation (Grant No. 4222001).

### References

- [1] Z. Younossi, F. Tacke, M. Arrese, B. Chander Sharma, I. Mostafa, E. Bugianesi, V. Wai-Sun Wong, Y. Yilmaz, J. George, J. Fan, M.B. Vos, Global perspectives on nonalcoholic fatty liver disease and nonalcoholic steatohepatitis, *Hepatology* 69 (2019) 2672–2682.
- [2] A. D'Hondt, E. Rubesova, H. Xie, V. Shamdasani, R.A. Barth, Liver fat quantification by ultrasound in children: a prospective study, *Am. J. Roentgenol.* 217 (2021) 996–1006.
- [3] E.L. Anderson, L.D. Howe, H.E. Jones, J.P. Higgins, D.A. Lawlor, A. Fraser, The prevalence of non-alcoholic fatty liver disease in children and adolescents: a systematic review and meta-analysis, *PLoS One* 10 (2015), e0140908.
- [4] J.B. Schwimmer, K.P. Newton, H.I. Awai, L.J. Choi, M.A. Garcia, L.L. Ellis, K. Vanderwall, J. Fontanesi, Paediatric gastroenterology evaluation of overweight and obese children referred from primary care for suspected non-alcoholic fatty liver disease, *Aliment. Pharmacol. Ther.* 38 (2013) 1267–1277.
- [5] H. Moran-Lev, S. Cohen, M. Webb, A. Yerushalmy-Feler, A. Amir, D.L. Gal, R. Lubetzky, Higher BMI predicts liver fibrosis among obese children and adolescents with NAFLD - an interventional pilot study, *BMC Pediatr.* 21 (2021) 385.
- [6] A.M. Pirmoazen, A. Khurana, A. El Kaffas, A. Kamaya, Quantitative ultrasound approaches for diagnosis and monitoring hepatic steatosis in nonalcoholic fatty liver disease, *Theranostics* 10 (2020) 4277–4289.
- [7] E.M. Brunt, C.G. Janney, A.M. Di Bisceglie, B.A. Neuschwander-Tetri, B.R. Bacon, Nonalcoholic steatohepatitis: a proposal for grading and staging the histological lesions, *Am. J. Gastroenterol.* 94 (1999) 2467–2474.
- [8] G. Cloutier, F. Destremes, F. Yu, A. Tang, Quantitative ultrasound imaging of soft biological tissues: a primer for radiologists and medical physicists, *Insights Imaging* 12 (2021) 127.
- [9] J. Park, J.M. Lee, G. Lee, S.K. Jeon, I. Joo, Quantitative evaluation of hepatic steatosis using advanced imaging techniques: focusing on new quantitative ultrasound techniques, *Korean J. Radiol.* 23 (2022) 13–29.
- [10] F. Destremes, G. Cloutier, Review of envelope statistics models for quantitative ultrasound imaging and tissue characterization, *Adv. Exp. Med. Biol.* 1403 (2023) 107–152.
- [11] Z. Zhou, Q. Zhang, W. Wu, Y.H. Lin, D.I. Tai, J.H. Tseng, Y.R. Lin, S. Wu, P.H. Tsui, Hepatic steatosis assessment using quantitative ultrasound parametric imaging based on backscatter envelope statistics, *Appl. Sci.* 9 (2019) 661.
- [12] Z. Zhou, D.I. Tai, Y.L. Wan, J.H. Tseng, Y.R. Lin, S. Wu, K.C. Yang, Y.Y. Liao, C.K. Yeh, P.H. Tsui, Hepatic steatosis assessment with ultrasound small-window entropy imaging, *Ultrasound Med. Biol.* 44 (2018) 1327–1340.
- [13] Z. Zhou, Q. Zhang, W. Wu, Y.H. Lin, D.I. Tai, J.H. Tseng, Y.R. Lin, S. Wu, P.H. Tsui, Hepatic steatosis assessment using ultrasound homodyned-K parametric imaging: the effects of estimators, *Quant. Imag. Med. Surg.* 9 (2019) 1932–1947.
- [14] T.Y. Chang, S.H. Chang, Y.H. Lin, W.C. Ho, C.Y. Wang, W.J. Jeng, Y.L. Wan, P.H. Tsui, Utility of quantitative ultrasound in community screening for hepatic steatosis, *Ultrasonics* 111 (2021), 106329.
- [15] Y.H. Chuang, C.S. Hsieh, M.W. Lai, C.C. Chen, H.C. Chao, H.Y. Yeh, H.H. Lai, P.H. Tsui, Detection of pediatric hepatic steatosis through ultrasound backscattering analysis, *Eur. Radiol.* 31 (2021) 3216–3225.
- [16] M.B. Vos, S.H. Abrams, S.E. Barlow, S. Caprio, S.R. Daniels, R. Kohli, M. Mouzaki, P. Sathya, J.B. Schwimmer, S.S. Sundaram, S.A. Xanthakos, NASPGHAN clinical practice guideline for the diagnosis and treatment of nonalcoholic fatty liver disease in children: recommendations from the expert committee on NAFLD (ECON) and the North American Society of Pediatric Gastroenterology, Hepatology and Nutrition (NASPGHAN), *J. Pediatr. Gastroenterol. Nutr.* 64 (2017) 319–334.
- [17] C.O. Mărginean, L.E. Meliț, D.V. Ghiga, M.O. Săsăran, The assessment of liver fibrosis in children with obesity on two methods: transient and two dimensional shear wave elastography, *Sci. Rep.* 9 (2019), 19800.
- [18] B.G. Jun, W.Y. Park, E.J. Park, J.Y. Jang, S.W. Jeong, S.H. Lee, S.G. Kim, S.W. Cha, Y.S. Kim, Y.D. Cho, H.S. Kim, B.S. Kim, S.Y. Jin, S. Park, A prospective comparative assessment of the accuracy of the FibroScan in evaluating liver steatosis, *PLoS One* 12 (2017), e0182784.
- [19] J.H. Lee, D. Kim, H.J. Kim, C.H. Lee, J.I. Yang, W. Kim, Y.J. Kim, J.H. Yoon, S.H. Cho, M.W. Sun, H.S. Lee, Hepatic steatosis index: a simple screening tool reflecting nonalcoholic fatty liver disease, *Dig. Liver Dis.* 42 (2010) 503–508.
- [20] L. Fedchuk, F. Nascimbeni, R. Pais, F. Charlotte, C. Housset, V. Ratzju, LIDO Study Group, Performance and limitations of steatosis biomarkers in patients with nonalcoholic fatty liver disease, *Aliment. Pharmacol. Ther.* 40 (2014) 1209–1222.
- [21] A.B. Mjelle, A. Mulabecirovic, R.F. Havre, K. Rosendahl, P.B. Juliusson, E. Olafsdottir, O.H. Gilja, M. Vesterhus, Normal liver stiffness values in children: a comparison of three different elastography methods, *J. Pediatr. Gastroenterol. Nutr.* 68 (2019) 706–712.
- [22] J. Zeng, X. Zhang, C. Sun, Q. Pan, W.Y. Lu, Q. Chen, L.S. Huang, J.G. Fan, Feasibility study and reference values of FibroScan 502 with M probe in healthy preschool children aged 5 years, *BMC Pediatr.* 19 (2019) 129.
- [23] V. Nobili, F. Vizzutti, U. Arena, J.G. Abraldes, F. Marra, A. Pietrobattista, R. Fruhwirth, M. Marcellini, M. Pinzani, Accuracy and reproducibility of transient elastography for the diagnosis of fibrosis in pediatric nonalcoholic steatohepatitis, *Hepatology* 48 (2008) 442–448.
- [24] Y.H. Lin, Y.L. Wan, D.I. Tai, J.H. Tseng, C.Y. Wang, Y.W. Tsai, Y.R. Lin, T.Y. Chang, P.H. Tsui, Considerations of ultrasound scanning approaches in non-alcoholic fatty liver disease assessment through acoustic structure quantification, *Ultrasound Med. Biol.* 45 (2019) 1955–1969.
- [25] P.H. Tsui, C.K. Chen, W.H. Kuo, K.J. Chang, J. Fang, H.Y. Ma, D. Chou, Small-window parametric imaging based on information entropy for ultrasound tissue characterization, *Sci. Rep.* 7 (2017), 41004.
- [26] Z. Zhou, J. Fang, A. Cristea, Y.H. Lin, Y.W. Tsai, Y.L. Wan, K.M. Yeow, M.C. Ho, P.H. Tsui, Value of homodyned K distribution in ultrasound parametric imaging of hepatic steatosis: an animal study, *Ultrasonics* 101 (2020), 106001.
- [27] J.S. Ko, J.M. Yoon, H.R. Yang, J.K. Myung, H. Kim, G.H. Kang, J.E. Cheon, J.K. Seo, Clinical and histological features of nonalcoholic fatty liver disease in children, *Dig. Dis. Sci.* 54 (2009) 2225–2230.
- [28] D.E. Kleiner, H.R. Makhlof, Histology of nonalcoholic fatty liver disease and nonalcoholic steatohepatitis in adults and children, *Clin. Liver Dis.* 20 (2016) 293–312.
- [29] Y. Wu, L. Lopez, M.P. Andre, R. Loomba, C.B. Sirlin, M.A. Valasek, M.A. Wallig, W.D. O'Brien, A. Han, Liver fat droplet dependency on ultrasound backscatter coefficient in nonalcoholic fatty liver, *IEEE Int Ultrason Symp* 1 (2020) 1–4.

- [30] A. Seth, S. Orkin, T. Yodoshi, C. Liu, L. Fei, J. Hardy, A.T. Trout, A.C. Arce Clachar, K. Bramlage, S. Xanthakos, M. Mouzaki, Severe obesity is associated with liver disease severity in pediatric non-alcoholic fatty liver disease, *Pediatr Obes* 15 (2020), e12581.
- [31] S.S. Bailey, M. Youssfi, M. Patel, H.H. Hu, G.Q. Shaibi, R.B. Towbin, Shear-wave ultrasound elastography of the liver in normal-weight and obese children, *Acta Radiol.* 58 (2017) 1511–1518.
- [32] Y.W. Tsai, Z. Zhou, C.A. Gong, D.I. Tai, A. Cristea, Y.C. Lin, Y.C. Tang, P.H. Tsui, Ultrasound detection of liver fibrosis in individuals with hepatic steatosis using the homodyned K distribution, *Ultrasound Med. Biol.* 47 (2021) 84–94.
- [33] E.G. Giannini, R. Testa, V. Savarino, Liver enzyme alteration: a guide for clinicians, *Can. Med. Assoc. J.* 172 (2005) 367–379.
- [34] S.B. Ahn, Noninvasive serum biomarkers for liver steatosis in nonalcoholic fatty liver disease: current and future developments, *Clin. Mol. Hepatol.* 29 (2023) S150–S156.
- [35] Y. Huang, Z. Wang, B. Liao, J.Y. Liang, L.Y. Zhou, F. Wang, W. Li, J.Y. Liu, X.Y. Xie, M.D. Lu, G.J. Liu, W. Wang, Assessment of liver fibrosis in chronic hepatitis B using acoustic structure quantification: quantitative morphological ultrasound, *Eur. Radiol.* 26 (2016) 2344–2351.